Earthquakes and Structures, *Vol. 19, No. 2 (2020) 79-90*
DOI: https://doi.org/10.12989/eas.2020.19.2.079

Seismic fragility curves using pulse-like and spectrally equivalent ground-motion records

Mitesh Surana*

Department of Civil Engineering, Indian Institute of Technology Ropar, Rupnagar – 140001, Punjab, India

(Received September 28, 2019, Revised July 15, 2020, Accepted August 7, 2020)

Abstract. 4- and 8-storey reinforced-concrete frame buildings are analyzed under the suites of the near-fault pulse-like, and the corresponding spectrally equivalent far-fault ground-motion records. Seismic fragility curves for the slight, moderate, extensive, and complete damage states are developed, and the damage probability matrices, and the mean loss ratios corresponding to the Design Basis Earthquake and the Maximum Considered Earthquake hazard levels are compared, for the investigated buildings and sets of ground-motion records. It is observed that the spectrally equivalent far-fault ground-motion records result in comparable estimates of the fragility curve parameters, as that of the near-fault pulse-like ground-motion records. As a result, the derived damage probability matrices and mean loss ratios using two suites of ground-motion records differ only marginally (of the order of ~10%) for the investigated levels of seismic hazard, thus, implying the potential for application of the spectrally equivalent ground-motion records, for seismic fragility and risk assessment at the near-fault sites.

Keywords: damage probability matrix; ground-motion; nonlinear response; reinforced-concrete frame buildings; seismic fragility; seismic risk

1. Introduction

The Indian Himalayan region, starting from Jammu and Kashmir in the North, to the Arunachal Pradesh in the North East is considered to be one of the most tectonically active regions of the world. The Indian Himalayas and its adjoining regions are seen from a geological perspective, relatively young geological formations, which produced several devastating earthquakes in the past century including, 1934 Nepal Bihar earthquake (M_w=8.0), 1950 Assam-Tibet earthquake (M_w=8.6), 1986 Dharamshala earthquake (M_w=5.5), 1991 Uttarkashi earthquake (M_w=6.8), 1999 Chamoli earthquake (M_w=6.8), 2005 Kashmir earthquake (M_w=7.6), 2011 Sikkim earthquake (M_w=6.9), and 2016 Manipur earthquake (M_w=6.7). This region is mostly characterized by high seismicity, with a majority of the underlying area falling under the category of the seismic zones IV and V, with an Effective Peak Ground Acceleration (EPGA) of 0.24 g and 0.36 g, respectively (BIS 2016a). The Indian Himalayan region has active faults located within a few kms away (typically ranging between 0-30 kms) from sites at many locations (e.g., Mussoorie site in Uttarakhand, located in close proximity of the Main Boundary Thrust). Ambraseys and Douglas (2000) reported that categorization of a near-fault site not only depends on the closest distance from the site to the fault rupture (r), but it also depends on magnitude of the earthquake. However, in literature, closest distances between the site to the fault rupture even up to 60 kms, and independent of the size of the earthquake event (i.e., magnitude) are frequently employed (e.g., Stewart *et al.* 2002, Bazzurro and Luco 2006, FEMA P695 2009) to categorize the near-fault sites. Thus, based on this categorization, many sites in the Indian Himalayan region fall under the category of the near-fault sites.

World-over ground motions recorded in the near-fault region, under some of the recent past earthquake events (e.g., 1994 Northridge earthquake, 1995 Kobe earthquake, and 1999 Chi-Chi earthquake) are distinctly noticeable, from those recorded in the far-fault region. Sometimes, at near-fault sites, high amplitude acceleration or velocity pulses are observed, which usually occurs in the fault normal component of the ground-motion record. These types of ground motions are classified as "near-fault pulse-like" ground motions. These strong pulses in ground motions are observed at the sites, where the rupture velocity is close to the shear wave velocity, and this effect is termed as "forward directivity effect" (Somerville *et al.* 1997). As a consequence of the presence of strong velocity pulses, a significant proportion of the energy of the ground-motion arrives in a single burst at the site, and usually at the beginning of the ground-motion record (Somerville *et al.* 1997). It has been noticed (e.g., Kumar *et al.* 2016) that the presence of these velocity pulses, in general lead to amplified spectral demands for spectral periods in close proximity to the pulse period (T_p). Further, in some cases, even for the very same ground-motion record, these pulse effects are observed to be very different in the different orientations of the ground-motion, and this effect is termed as "directionality effect" (Shahi and Baker 2014).

Due to the combined effects of the scarcity of the ground-motion recording stations, and limited duration of the installation of a dense network of strong-motion

*Corresponding author, Assistant Professor
E-mail: msurana@iitrpr.ac.in

http://www.techno-press.com/journals/was&subpage=7
ISSN: 2092-7614 (Print), 2092-7622 (Online)

recording stations (e.g., mostly installed after 2004, please see, Kumar *et al.* 2012) for the Indian Himalayan region, very limited records with these pulse-like characteristics have been identified explicitly. Kumar *et al.* (2016) identified the presence of the strong velocity pulses in a very few of the ground motions recorded in the Himalayan region (e.g., 1986 Dharamshala earthquake at 'Shahpur' station, 1991 Uttarkashi earthquake at 'Bhatwari' station, 1999 Chamoli earthquake at 'Gopeshwar' station) in the recent past. As a result of the aforementioned facts, the likelihood of the occurrence of the near-fault pulse-like ground motions cannot be completely disregarded, in the context of the Indian Himalayan region.

Significant research efforts have been given in the recent past to characterize the pulse-like ground motions (e.g., Baker 2007, Zamora and Riddell 2011, Chang *et al.* 2019). Ansari *et al.* (2018) evaluated the effect of vertical component of near-fault ground motions on seismic demand experienced by columns. Some studies (e.g., Mavroeidis *et al.* 2004, Bazzurro and Luco 2006, Tothong and Cornell 2008) identified the effects of pulse-like ground-motion characteristics (i.e., the amplitude of the pulse, the pulse period, T_p, and the number of half cycles) on the structural response, whereas, the others (e.g., Ruiz-Garcia 2011, Iervolino *et al.* 2012) focused on estimation of the inelastic displacement ratios for the pulse-like ground motions and compared seismic response of moment resisting frame buildings, under the pulse-like and the far-fault (ordinary) ground-motion records (e.g., Akkar *et al.* 2005, Alavi and Krawinkler 2004, Mansouri *et al.* 2019). These studies (e.g., Akkar *et al.* 2005, Alavi and Krawinkler 2004, Mansouri *et al.* 2019) identified that the pulse-like ground motions impose higher demands on the structures, as compared to the far-fault ground motions. Champion and Liel (2012) assessed collapse risk of reinforced-concrete (RC) frame buildings subjected to near-fault pulse-like ground motions, and showed that pulse-like ground motions exhibit on average 6% collapse risk in 50 years, which was observed to be six times higher than targeted risk for seismic design of ordinary buildings, in the United States building code. One of the major reasons for the aforementioned observations could be attributed to characteristically different spectral shape of the pulse-like ground motions as compared to their counterpart far-fault ground motions.

Recent studies (e.g., Baker and Cornell 2006, Haselton *et al.* 2011) showed the severe impact of the spectral shape of the ground-motion records in the seismic fragility assessment. For example, FEMA P695 (2009) suggested the enhancement in the collapse capacity up to 60%, due to spectral shape effects, for some sites in the United States. To consider the effect of spectral shape of ground-motion records in structural response estimation and seismic fragility assessment, the advanced ground-motion selection techniques such as Conditional Mean Spectrum (CMS, Baker 2011), Conditional Spectrum (CS, Jayaram *et al.* 2011), and Generalized Conditional Intensity Measure (GCIM, Bradley 2010) consistent with the site-specific seismic hazard analysis have been developed over the past decade. Most of these ground-motion selection techniques are structure, and site-specific in nature. As an alternative to these ground-motion selection techniques, Eads *et al.* (2015, 2016) developed the advanced ground-motion intensity measure (IM), e.g., $S_{a,avg}$ defined as the geometric mean of spectral acceleration over a period range between $0.2T$ and $3T$ (here, T is the fundamental period of the building). These ground-motion selection techniques were developed for the far-fault sites, and later on modified to select ground motions, even for the near-fault sites with pulse-like effects (e.g., Chioccarelli and Iervolino 2013, Almufti *et al.* 2015). Recently, Kohrangi *et al.* (2019) underlined that accuracy and practicality in the near-fault seismic risk assessment can be ensured, if pulse-like ground motions are selected based on the T_p distribution obtained from the hazard disaggregation at given value of $S_{a,avg.}$

The existing studies related to development of the seismic fragility functions for RC frame buildings (e.g., Haldar and Singh 2009, Haldar *et al.* 2012) for the Indian Himalayan region are based on nonlinear static analysis based 'Capacity Spectrum Method' and do not account for the special characteristics (e.g., the pulse period, T_p and the spectral shape) of the pulse-like ground-motion records. Further, the reported studies in the literature are limited to the comparison of the drift demands (Akkar *et al.* 2005, Alavi and Krawinkler 2004) and the collapse risk assessment (Champion and Liel 2012). Further, the above discussed ground-motion selection techniques for choosing the near-fault pulse-like ground motions (e.g., Chioccarelli and Iervolino 2013, Kohrangi *et al.* 2019) are difficult to implement in the regional seismic fragility and risk assessment studies, particularly, due to following reasons: (i) multiple constraints for selection of ground motions (e.g., accounting for the spectral shape through $S_{a,avg}$ dependent on the spectral period of interest, and at the same time maintaining T_p distribution), (ii) selection of ground motions for multiple hazard levels (to capture full probabilistic distribution of IM and engineering demand parameter (EDP) for various damage states, e.g., slight, moderate, extensive and complete), and (iii) limited availability of the recorded near-fault pulse-like ground motions. In addition, only very limited regional ground-motion prediction equations are available so far for the advanced IM such as $S_{a,avg}$ (which accounts for the spectral shape of the ground-motion). Therefore, performing seismic hazard analysis in terms of $S_{a,avg}$ is also not possible in all the cases, thus, also restricts the applicability of the available ground-motion selection procedures, based on $S_{a,avg}$ in the most parts of the world. As a result of these limitations, the simple and alternative methods for practical application in seismic fragility and risk assessment for the near-fault sites are to be investigated and explored.

Based on the aforesaid discussions, the present study aims to investigate the potential of spectrally equivalent ground motions in seismic fragility assessment at the near-fault sites, as an alternative to the near-fault pulse-like ground motions. Accordingly, the regular in configuration, RC moment resisting frame buildings with 4- and 8-storeys, with different plan dimensions in the two orthogonal directions are considered. These buildings are analyzed under two different suites of the ground-motion records, i.e., the near-fault pulse-like ground-motion record suite and the corresponding spectrally equivalent ground-motion record suite, with each suite having 192 horizontal components of the ground motions. The seismic fragility curves for 'slight', 'moderate', 'extensive' and 'complete' damage states are developed, in terms of two different physical ground-motion IMs, i.e., $S_a(T, 5\%)$, and $S_{a,avg}$ $(0.2T\text{-}3T, 5\%)$, hereafter referred as S_a and $S_{a,avg}$ respectively. The obtained sets of seismic fragility curves from both the suites of ground-motion records are compared. The developed fragility curves in terms of Sa for investigated cases of the buildings are further used to estimate and compare the damage probability matrices (DPMs) and the mean loss ratios (MLR), corresponding to the Design Basis Earthquake (DBE) and the Maximum Considered Earthquake (MCE) hazard levels.

2. Seismic fragility assessment

In the literature, a variety of methods have been developed for seismic fragility assessment. The developed methods differ from each other based on the fact that how the correlation between the ground-motion IM and physical damage is considered. These methods of seismic fragility assessment includes: (i) the empirical methods (e.g., Rossetto and Elnashai 2003, Jaiswal *et al.* 2011, Maqsood *et al.* 2016) which mostly relies on the collected damage data from the past earthquakes, in conjunction with intensity scales such as Modified Mercalli Intensity (MMI; Wood and Neumann 1931) to include the severity of ground-motion records, and (ii) the analytical methods (e.g., Singhal and Kiremidjian 1996, Rossetto and Elnashai 2005), which can vary from simple nonlinear static method (e.g., Capacity spectrum method) to the cumbersome nonlinear dynamic analysis based stripe analyses (e.g., multiple stripe analysis), which generally uses the physical ground-motion parameters (e.g., peak ground acceleration, PGA, 5%-damped spectral acceleration at the fundamental mode period, S_a, etc.) as the ground-motion IM. In absence of the damage data from the past earthquakes or limited availability of damage data, a combination of the empirical and analytical approach can also be implemented, and often referred as hybrid approach (e.g., Barbat *et al.* 1996, Kappos *et al.* 1998, Lang 2013).

Though, empirical methods are considered to be the most practical and suitable method of seismic fragility assessment, the unavailability of the damage data from the past earthquakes in the Indian Himalayan region and its systematic documentation makes it very challenging for its practical application (Haldar and Singh 2009). Thus, the analytical methods of fragility assessment serve as one of the viable option for the regional seismic risk assessment. The analytical methods of seismic fragility assessment involve the application of the one of the following approaches on the estimated IM and EDP relationships from dynamic structural analyses: (i) Method of Least Square (LS), (ii) Method of Maximum Likelihood Estimation (MLE), and (iii) Method of Sum of Squared Error (SSE), to establish a probabilistic relationship between the ground-motion IM and the EDP. In case of the LS approach, the relationship between IM and EDP is pre-defined in the form of a power law, whereas, the MLE approach does not assume any pre-defined relationship, and thereby, MLE approach is considered to be more suitable for the cases where the dynamic analysis results are constrained (Gehl *et al.* 2015). Further, in case of the LS approach, the assumed power law can also vary over the various damage states e.g. piece-wise LS regression for different damage states (Carausu and Vulpe 1996). Furthermore, the LS approach utilizes the complete information from the dynamic analysis, whereas the MLE utilizes the information from dynamic analyses in the form of binary outputs only, e.g. damage or no damage (Kim and Shinozuka 2004, Zenter 2010), and thus, results in the loss of the exact information, with respect to the extent of damage. Gehl *et al.* (2015) reported that using the LS approach, the convergence of the analytical fragility curve to a reference fragility curve can be achieved, even using only a few dozen of ground-motion records.

In the present study, to obtain the seismic fragility curve parameters for different damage states, ground-motion suites and ground-motion IMs, the IM-EDP response obtained for nonlinear dynamic analyses is used in conjunction with piece-wise LS regression method. The boundaries of different damage states are defined based on the maximum inter-storey drift thresholds (as defined later in this article). For example, to perform piece-wise LS regression for 'moderate' damage state, IM-EDP pairs (in each of the investigated cases atleast 40 in number) falling between the maximum inter-storey drift thresholds corresponding to the 'slight' and 'extensive' damage state are considered, and the median and standard deviations are computed.

3. Numerical study

Extensive field surveys conducted in the two popular tourist destinations (i.e., Mussoorie and Nainital) of the Indian Himalayan region reveals that RC frame buildings is the most often observed building typology (Surana *et al.* 2018) in this region. Accordingly, to conduct the present study, RC moment-resisting frame buildings, with a generic building plan representative of the typical (average) characteristics (in terms of the number of bays, bay widths etc.) of existing housing stock in the Indian Himalayan region is chosen (Surana 2019) and the corresponding plan details are shown in Fig. 1. Buildings with 4- and 8-storeys, (classified under the category of mid-rise and high-rise, respectively, as per the definition of FEMA 2002) are considered in the present study. Based on the average height of the storeys in the typical existing housing stock in the Indian Himalayan region (Surana *et al.* 2018), the storey height of 3.30 m is considered for all the storeys.

Numerical structural models of the considered RC moment-resisting frame buildings are developed in the proprietary Finite Element package ETABS 2016 (CSI 2016). 3D frame elements are used to model beams and columns, and slabs are defined as rigid diaphragms. To consider the cracked section stiffness for beams and

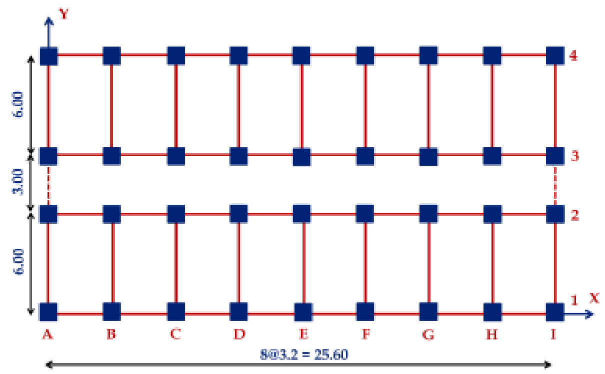

Fig. 1 Plan of the representative buildings chosen for the present study. All dimensions reported in the figure are in meters. The broken lines in the floor plan along Y direction represent the boundaries of floor slab, which are assumed to be rigid in its own plane

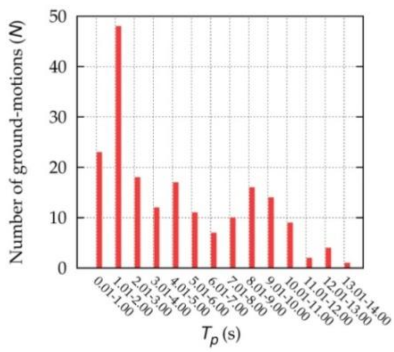

Fig. 2 Pulse period distribution for the chosen set of pulse-like ground motions

columns, ASCE 41 (2013) guidelines are used. Gravity loads on the buildings are modelled based on the guidelines recommended in the Indian Standards (BIS 1987a, 1987b). The buildings are designed for Indian seismic zone IV (at rock site) as Special Moment Resisting Frames (with a 'response reduction factor' of 5) and detailed as per the recommendations of the Indian Standard (BIS 2016b). The design seismic hazard in Indian seismic zone IV corresponds to short-period design spectral acceleration, S_{DS} = 0.45 g and design spectral acceleration at 1s, S_{D1} = 0.18 g, respectively. The considered design spectral ordinates for the investigated buildings are comparable with seismic design category C in the United States. The design base shear coefficients for 4- and 8-storey buildings are 0.065 and 0.040, respectively. P-delta effects (second order) are considered in both analysis and design. The sizes of the structural elements (i.e., beams and columns) are chosen consistent with the design practice in the high seismic zones of India, i.e., Northern and Northeastern India, and structural members are proportioned to result in longitudinal reinforcement between 0.75 - 1.5% (on each face) for beams, and 2 - 4% for columns. The modal analysis of the considered buildings resulted in the fundamental (translational mode) periods of 4-storey building equal to 1.21s and 1.77s in the X and Y directions, respectively, whereas, equal to 2.60s and 4.10s, for 8-stroey building, in the X and Y directions, respectively.

3.1 Nonlinear modelling

The considered RC moment-resisting frame buildings are designed and detailed for capacity shear provisions, ensuring the flexural failure of the structural elements (i.e., beams and columns), under seismic action. Accordingly, in the present study, the flexural failure of the beams and columns is modelled using the concentrated hinges, at the ends of the structural elements. The moment (M3) hinges for beams, and axial-flexure interacting (P-M2-M3) hinges for columns are assigned. The backbone curve parameters for both M3 and P-M2-M3 hinges are obtained from ASCE 41 (2013) guidelines. As ASCE 41 define backbone curves based on cyclic envelopes, and hence, these curves inherently include the strength degradation effects under cyclic loadings. Further, to consider the stiffness degradation effects in the successive cycles, energy based degrading hysteretic model has been used. The corresponding model parameters to consider the energy dissipation (in the pre- and post-capping range of the backbone curves) are obtained from an earlier study (Surana *et al.* 2018). The additional details related to the calibration and derivation of the degrading hysteretic model parameters is available in Surana *et al.* (2018).

3.2 Ground-motion selection

The objective of the present study is to compare the seismic fragility functions, discrete damage probabilities, and loss ratios obtained from the near-fault pulse-like ground-motion suite with the corresponding spectrally equivalent far-fault suite and to investigate whether the spectral equivalency alone could serve as a criterion for the selection of ground-motion records for seismic fragility assessment in the near-fault sites. Accordingly, in the present study, two different ground-motion record suites, each comprising of 192 ground motions as identified in an earlier study (Kohrangi *et al.* 2019) are chosen. The first suite corresponds to the near-fault pulse-like ground motions, whereas, the second suite corresponds to the spectrally equivalent (i.e., the spectral shape of the far-fault ground-motion record is similar and comparable to the corresponding near-fault pulse-like ground-motion record, in the period range of interest) far-fault ground motions. It is to be noted here that the pulse-like record suite consist of natural (unscaled) records, whereas, the spectrally equivalent records consist of the amplitude scaled records. The spectral equivalency of the ground-motion records is considered for the spectral periods between 0.05-6.00s (Kohrangi *et al.* 2019). The chosen range of the spectral periods appropriately considers the typical range of the fundamental periods of the investigated set of buildings, as well as the expected elongation in the fundamental period of the buildings, due to inelastic response.

The moment magnitude, the closest distance, and the PGA of the chosen set of pulse-like ground motions range between 5.00-7.60, 0.1-92.7 kms, and 0.05-1.49 g, respectively, whereas, the corresponding values in case of

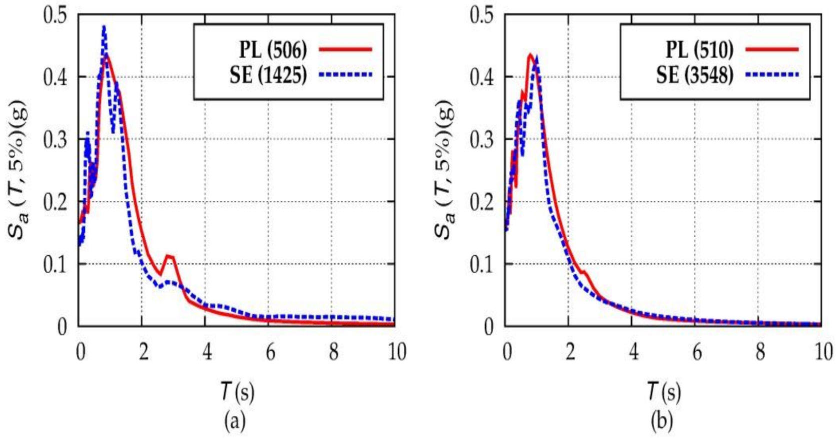

Fig. 3 Comparisons of the response spectra of the near-fault pulse-like (PL) and the corresponding spectrally equivalent (SE) far-fault ground motions. The number in the parentheses represents the PEER NGA sequence number of the respective ground motions

the spectrally equivalent ground motions range between 6.00-7.90, 7.57-198.62 kms, and 0.05-1.26 g, respectively. It is to be noted here that the reported values of PGA in case of the spectrally equivalent ground-motion records correspond to scaled ground motions. The scale factors for these spectrally equivalent ground motion records vary between 0.21-4.96, with an average value of 2.54. The near-fault pulse-like ground motions have the presence of velocity pulses with a pulse period varying between 0.26-13.12s. The bin-wise distribution of the pulse period and number of ground motions in each of the considered bins is shown in Fig. 2. The additional details (e.g., site class, horizontal component H1 or H2, etc.) of the chosen sets of the ground-motion records are available in Kohrangi *et al.* (2019).

Fig. 3 presents a comparison of the 5%-damped elastic acceleration response spectra for the near-fault pulse-like (PL) and the corresponding spectrally equivalent (SE) ground-motion records for example cases. It is evident that the spectrally equivalent records (scaled) compared on one-to-one basis are comparable in spectral shape and magnitude with their corresponding pulse-like ground-motion records, in the spectral period range between 0.05-6.00s. A similar degree of the comparison also exist for the other ground motions as well, however, the plots corresponding to those cases are not reported here for brevity.

3.3 Nonlinear dynamic analysis

The developed structural models are subjected to uni-directional earthquake excitations using both the suites of ground-motion records, and the structural response in terms of the EDP (i.e., maximum inter-storey drift ratio, MIDR) is obtained for each of the ground-motion record, in both the record suites. To conduct the nonlinear dynamic analyses, Viscous damping in the building structure is assumed to be 5%, and defined as Rayleigh damping corresponding to the fundamental mode and the mode resulting a cumulative modal mass participation of 95%, in the direction of excitation.

4. Structural response cloud and fragility curve parameters

Nonlinear dynamic analyses using the near-fault pulse-like and the spectrally equivalent ground-motion record suites are conducted and the structural response is presented in the form of the ground-motion IM and EDP. Figs. 4 and 5 present the clouds of the structural response of the investigated 4- and 8-storey buildings, in both directions (i.e., X and Y), using two different ground-motion IMs, i.e., S_a and $S_{a,avg}$, respectively. It can be observed that clouds of the structural response are well spread in the IM-EDP plane, and some of the ground motions even caused collapse (shown corresponding to a drift ratio of 8%, Figs. 4 and 5) of the investigated set of buildings. In case, when S_a is chosen as the ground-motion IM, the dispersion in IM-EDP plane is smaller for MIDR's up to 2% (Fig. 4), and it further increases with an increase in the MIDR. On the other hand, in case of the $S_{a,avg}$, the dispersion in IM-EDP plane is more or less uniform throughout the range of the MIDR's. The observed dispersion in case of $S_{a,avg}$ is somewhat lesser for higher values of MIDR's (greater than 3%), when compared with the corresponding dispersion, while S_a is chosen as the ground-motion IM. These observations can be attributed to the facts that in case of the lower MIDR's (e.g., up to 1%) the structural response is nearly elastic or moderately inelastic. As all the investigated buildings are the fundamental mode dominated structures, their response is well predicted by S_a, thus, resulting a smaller dispersion. With an increase in the ground-motion intensity, the dynamic behaviour of the buildings gets affected by: (i) an increase in the contribution of the higher modes of vibration, and (ii) elongation in the fundamental period of the building. As a result, for the severely inelastic response of the building structure (e.g., 'extensive' and 'complete' damage states), the ground-motion IM accounting for the spectral ordinates corresponding to higher modes as well as the elongated period, in general, results the smaller dispersion.

The fragility curve parameters for all the buildings are estimated for the different damage states (i.e., 'slight',

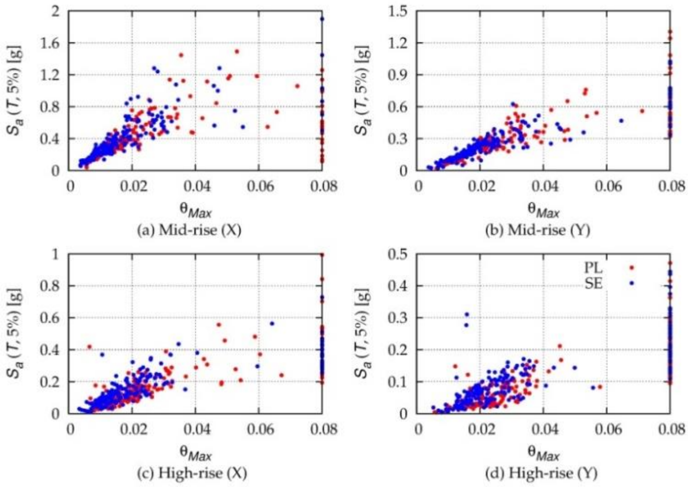

Fig. 4 Clouds of the structural response of the considered building archetypes for the near-fault pulse-like (PL) and the corresponding spectrally equivalent (SE) far-fault ground motions. The ground motions intensities which caused 'collapse' of the considered archetypes are shown at an MIDR of 8%

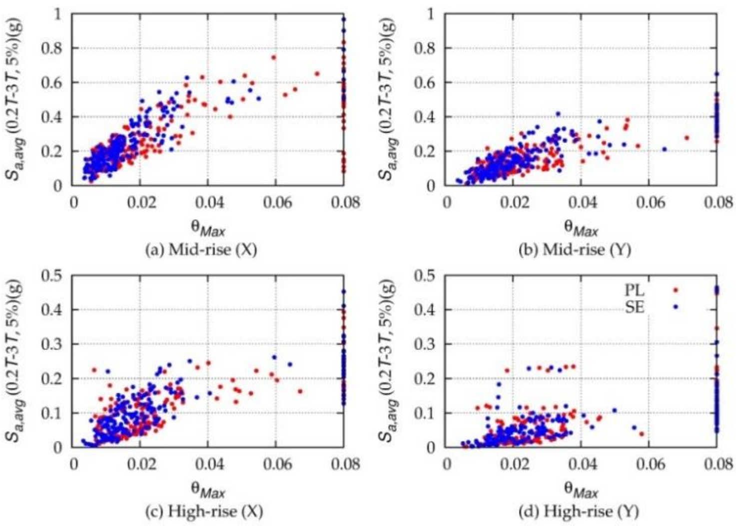

Fig. 5 Clouds of the structural response of the considered building archetypes for the near-fault pulse-like (PL) and the corresponding spectrally equivalent (SE) far-fault ground motions. The ground motions intensities which caused 'collapse' of the considered archetypes are shown at an MIDR of 8%

'moderate', 'extensive' and 'complete'), using both the ground-motion suites and in terms of both the ground-motion IMs, i.e., S_a and $S_{a,avg}$. To estimate the fragility curve parameters, the piece-wise LS regression technique is applied on the obtained IM-EDP pairs. The median values of the maximum inter-storey drift thresholds for different damage states are defined based on the corresponding values defined in FEMA (2002), as listed in Table 1. As the piece-wise LS regression allows both the power law relationship between ground-motion IM and EDP and the dispersion, to vary for different damage states, accordingly, the standard deviation of the error term is computed by using a piece-wise LS regression over various damage states. The seismic fragility curve parameters are computed using the corresponding power law relationship as

$$\ln(EDP) = a\ln(IM) + \ln(b), S.d. = \beta_{\varepsilon} \tag{1}$$

The median demand (α_{dsi}) and its dispersion (β_{dsi}) for each assumed threshold (d_{si}), are obtained as

$$\alpha_{ds_i} = \exp\left(\ln\left(\frac{ds_i}{b}\right)/a\right) and \beta_{ds_i} = \frac{\beta_{\varepsilon}}{a} \tag{2}$$

Table 2 presents the derived fragility curve parameters (α_{dsi} and β_{dsi}) using the method of Least Squares after correcting as per recommendations of FEMA (2015) for the considered 4- (mid-rise) and 8-storey (high-rise) buildings, investigated in the present study. The adopted correction procedure (FEMA 2015) to the seismic fragility curve parameters modifies the median value of IM for a given damage state and recommends to use average value of the dispersion (obtained considering all the damage states together), and thus ensures that two seismic fragility curves do not intersect with each

Table 1 Threshold values of the maximum inter-storey drift ratios for different damage states

Building Height	Damage states			
	Slight	Moderate	Extensive	Complete
Mid-rise	0.33%	0.67%	2.00%	5.33%
High-rise	0.25%	0.50%	1.50%	4.00%

Table 2 Fragility curve parameters for the considered buildings

Record Type	Building Height	Direction	IM	α_{dsi} Slight	α_{dsi} Moderate	α_{dsi} Extensive	α_{dsi} Complete	β_{dsi} All damage states
Near-fault pulse-like records	Mid-rise	X	S_a	0.055	0.156	0.500	0.505	0.34
			$S_{a,avg}$	0.048	0.121	0.303	0.360	0.44
		Y	S_a	0.016	0.047	0.201	0.399	0.26
			$S_{a,avg}$	0.017	0.038	0.123	0.289	0.42
	High-rise	X	S_a	0.022	0.034	0.101	0.268	0.51
			$S_{a,avg}$	0.022	0.028	0.065	0.177	0.66
		Y	S_a	0.001	0.003	0.028	0.094	0.51
			$S_{a,avg}$	0.001	0.003	0.020	0.072	0.84
Spectrally equivalent far-fault records	Mid-rise	X	S_a	0.078	0.156	0.463	0.743	0.25
			$S_{a,avg}$	0.056	0.111	0.298	0.602	0.33
		Y	S_a	0.019	0.054	0.204	0.428	0.25
			$S_{a,avg}$	0.018	0.038	0.132	0.301	0.35
	High-rise	X	S_a	0.010	0.024	0.110	0.268	0.43
			$S_{a,avg}$	0.005	0.015	0.073	0.182	0.53
		Y	S_a	0.002	0.005	0.036	0.123	0.56
			$S_{a,avg}$	0.002	0.004	0.023	0.074	0.68

other (Surana *et al.* 2020). The estimated fragility curve parameters for all the investigated buildings are reported for both the directions (X and Y) and in terms of both the ground-motion IMs, i.e., S_a and $S_{a\text{-}avg}$. It can be observed that the median capacities obtained for different damage states using two different suites of the ground-motion records are in reasonable agreement for all the buildings, excepting the case of 4-storey (mid-rise) building in the X direction, and particularly for the complete damage state. One of the major reasons for this inconsistency could be the wide dispersion in the IM-EDP plane (Fig. 4(a)) corresponding to this damage state, thus, resulting a poor piece-wise power law relationship between IM and EDP. The dispersion in pulse-like and spectrally equivalent ground motions are well comparable, especially, for the slight and the moderate damage states, whereas, a higher dispersion is obtained in case of the pulse-like ground motions, especially, for the extensive and the complete damage states, when compared with the corresponding values obtained for spectrally equivalent ground motion records. As average values of dispersion are reported in Table 2 (as per the correction procedure of FEMA 2015), therefore, the pulse-like ground motions set results in general higher record-to-record variability, as compared to the corresponding estimates, obtained using the spectrally equivalent set of ground-motion records.

It is reported (FEMA P695 2009, Meslem *et al.* 2014) that in addition to the record-to-record variability (β_{dsi}), there exist several sources of variabilities which are to be further considered in the seismic fragility assessment. These sources of variabilities include: (i) the modelling variability, (ii) the test data variability, (iii) the design requirements variability, and (iv) the variability in the prediction of the median damage state thresholds. In the present study, the modelling, the test data, and the design requirement variabilities are taken based on the recommendations of FEMA P695 (2009). Each of the corresponding values is taken as 0.20, based on the assumption of having a good confidence in the robustness and completeness in the test data, the modelling, and the design requirements for the considered RC frame buildings, as those are representative of Special Moment Resisting Frames. The variability in the estimation of the threshold of the damage states is taken as 0.40, based on the study by Meslem *et al.* (2014). All these sources of variabilities are considered to be independent and combined with record-to-record variability (Table 2) using the square root of sum of squares (SRSS) to estimate the total variability. It is observed that when all the sources of variabilities are combined, the higher record-to-record variability (β_{dsi}) observed in case of pulse-like ground motions is suppressed by the other sources of variabilities, discussed in this section. As a result, the 'average' values of the total variability for the investigated structural systems, and height ranges typically range between 0.58-1.00 for various damage states, with an average value of 0.71. The estimated values of the total variability (after combining all sources of variabilities) in the present study (even for the near-fault pulse-like and the spectrally equivalent ground motions) are in reasonable agreement with earlier studies and literature (e.g., Kappos and Panagopoulos 2010, FEMA P58 2015), which suggested total variability typically in the range of 0.60-0.70 (e.g., Kappos and Panagopoulos 2010) for well configured (regular) structures.

Figs. 6 and 7 present the seismic fragility curves derived

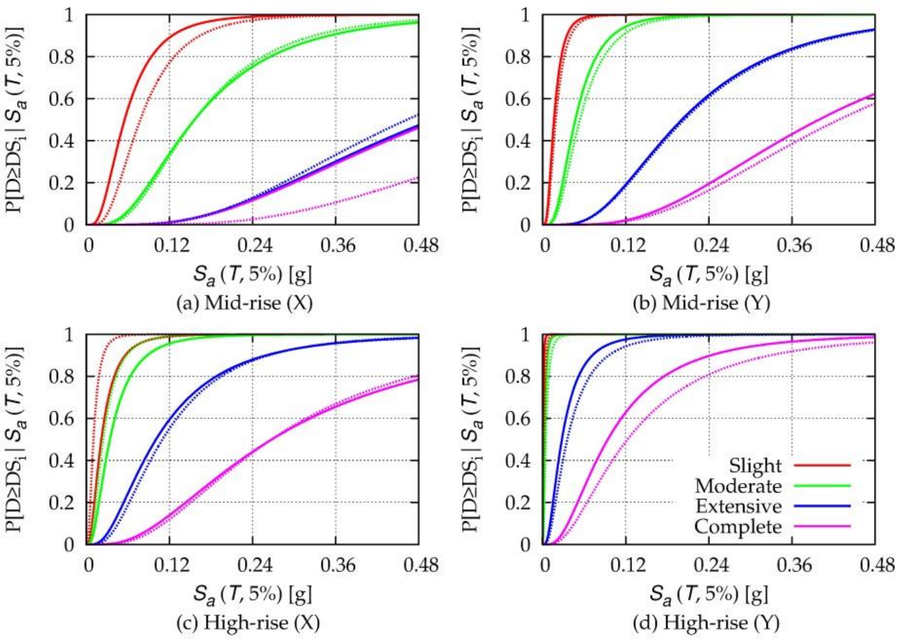

Fig. 6 Fragility curves of the considered building archetypes for the near-fault pulse-like (PL) and the corresponding spectrally equivalent (SE) far-fault ground motions. The firm lines correspond to the near-fault pulse-like ground motions, whereas the dotted lines correspond to the spectrally equivalent far-fault ground motions

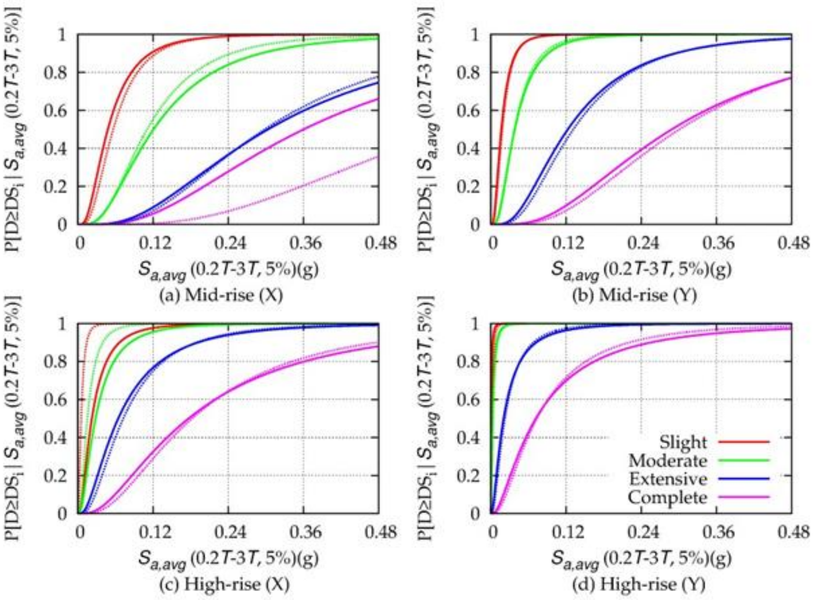

Fig. 7 Fragility curves of the considered building archetypes for the near-fault pulse-like (PL) and the corresponding spectrally equivalent (SE) far-fault ground motions. The firm lines correspond to the near-fault pulse-like ground motions, whereas the dotted lines correspond to the spectrally equivalent far-fault ground motions

using the estimated values of median thresholds and total variabilities in the present study. The seismic fragility curves are plotted in terms of two different physical ground-motion IMs i.e., S_a and $S_{a,avg}$ and for all the damage states. The fragility curves in firm lines correspond to the near-fault pulse-like ground motions record suite, whereas, the fragility curves in dotted lines correspond to the spectrally equivalent far-fault ground motions record suite. It can be observed that the derived fragility curves using both the suites of ground motions are in close agreement for all the damage states, except for extensive and complete damage states, in case of 4-storey mid-rise building in the X direction. As explained earlier, this observation can be attributed to relatively larger scatter in IM and EDP for these damage states, particularly, in case of the pulse-like ground motions. The presented observations not only highlight that the spectrally equivalent ground motions could serve as an alternative to the pulse-like ground motions for the near-fault sites, but it also highlight that comparable estimates of the predicted damage can be obtained, even for the near-fault sites, by choosing an IM like S_a, for which a number of ground-motion prediction models are available world-wide.

5. Damage probability matrices and mean loss ratio

To further study the effects of chosen sets of ground-motion records on the estimated physical damage, the damage probability matrices are computed for the DBE and MCE levels of seismic hazard for Indian seismic zone IV (at the Mussoorie site), using the seismic fragility curves developed in the present study. All the estimates are reported based on the seismic fragility curves developed using S_a as the ground-motion IM for both the suites of the ground motions. S_a for DBE and MCE hazard is computed based on the design response spectrum recommended in the Indian seismic design code (BIS 2016a).

Fig. 8 presents a comparison of the discrete damage probabilities obtained for the DBE and the MCE hazard (at Mussoorie site) using the near-fault pulse-like and the corresponding spectrally equivalent ground-motion records. It can be observed that the obtained estimates of the discrete damage probabilities are well comparable. In case of the DBE level of seismic hazard, the most of the damage is concentrated in the 'slight' and 'moderate' damage states, (as the structural response is expected to be nearly elastic to moderately inelastic), whereas, in case of the MCE level of seismic hazard, the estimated damage is mostly concentrated in the 'moderate' and 'extensive' damage states (as the structural response is expected to be moderate to severely inelastic).

In literature, excepting for the 'collapse' (in the present study the 'complete' damage state definition has been adopted based on FEMA (2002), which include both the 'partial' as well as 'total collapse') damage state, the appropriate values of the discrete damage probabilities for other damage states are not available. For example, FEMA P695 (2009) suggests 10% conditional probability of collapse (average value for a group of buildings), at the MCE hazard level to be adequate, from the 'collapse safety' perspective. The estimated (average) values of the conditional probability of the 'complete' damage at the MCE hazard are within the limits suggested by FEMA P695 (2009), implying acceptability of the design provisions of the Indian seismic design codes, at the design seismic hazard. However, in case of 8-storey building (e.g., Y direction), especially, while subjected to the near-fault pulse-like ground-motion suite, the estimated collapse probability at the MCE hazard is observed to be significantly higher (i.e., 29%, Fig. 8) as compared to that obtained from the spectrally equivalent ground-motion suite (i.e., 18%).

To quantify the impact of using spectrally equivalent ground motions as an alternative to the near-fault pulse-like ground motions, for the seismic risk assessment at the near-fault sites, the MLR estimated based on damage estimates obtained using the near-fault pulse-like and the corresponding spectrally equivalent ground-motion record suites, for the investigated buildings are compared for the DBE and the MCE hazard levels. One of the greatest advantages of using MLR lies in the fact that the effects of discrete damage probabilities for different damage states are combined in a single metric, thus it provides a more meaningful way of comparison of seismic loss associated with a building archetype. The MLR for the investigated buildings, for a given level of seismic hazard is computed using Eq. (3) as:

$$MLR = \left(\frac{\sum_{i=1}^{N} P(D = DS_i).EL_i}{\sum_{i=1}^{N} P(D = DS_i)} \right) \tag{3}$$

where, $P(D=DS_i)$ is the probability of experiencing the discrete damage state i for any given hazard level of interest, and EL_i is the ratio between the cost for repairing the specific damage state i to the building's replacement cost. In the present study, the fractions of the economic loss corresponding to the slight, moderate, extensive, and complete damage states are taken as 2%, 10%, 50% and 100% (in terms of building's replacement cost), respectively, as per the recommendations of HAZUS (FEMA 2002).

Fig. 9 presents a comparison of the estimated MLRs for all the investigated buildings, using two different suites of the ground-motion records, at two different seismic hazard levels (i.e., DBE and MCE), and choosing S_a as an IM. It can be observed that the use of the spectrally equivalent ground-motion records lead to comparable estimates of MLR for the DBE hazard, with a maximum underestimation of about 8% only. With an increase in seismic hazard level (i.e., MCE), the MLR is underestimated by about 13% for the investigated set of RC frame buildings. The observed differences in MLR obtained using two different suites considered in the present study can be considered to be marginal and acceptable, thereby, showing a potential for the applicability of the spectrally equivalent ground-motion records in seismic fragility and loss assessment for the near-fault sites.

6. Conclusions

Nonlinear dynamic analyses have been conducted on 4- and 8-storey RC moment-resisting frame buildings, using the suites of the near-fault pulse-like and the corresponding spectrally equivalent far-fault ground-motion records. The derived fragility functions, and corresponding damage probability matrices, and mean loss ratios, obtained using the two suites are compared to assess the applicability of the spectrally equivalent ground-motion records in the seismic fragility and risk assessment in the near-fault sites. The major findings of this study are summarized below:

- The spectrally equivalent ground motions results in comparable estimates of the median capacities associated with the various damage states, when

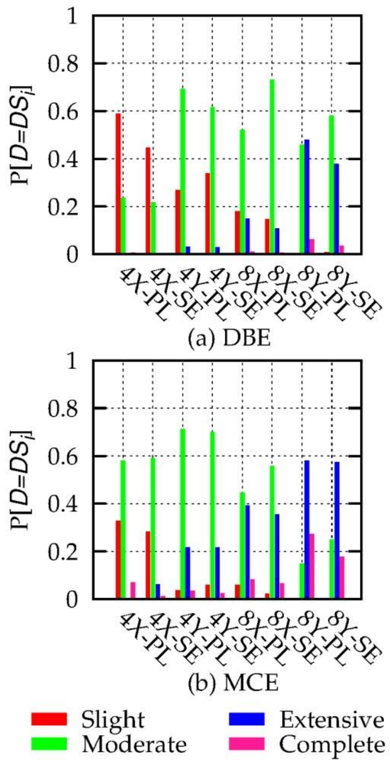

Fig. 8 Comparison of the damage probability matrices estimated using the derived fragility curves for the near-fault pulse-like (PL) and the corresponding spectrally equivalent (SE) ordinary ground motions, corresponding to the DBE and the MCE hazard levels

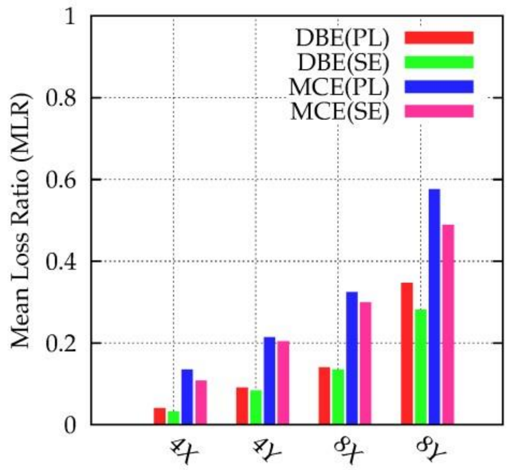

Fig. 9 Comparison of the mean loss ratio estimated using the derived fragility curves for the near-fault pulse-like (PL) and the corresponding spectrally equivalent (SE) ordinary ground motions, corresponding to the DBE and the MCE hazard levels

compared with their counterpart's near-fault pulse-like ground motions.

• The spectrally equivalent ground motions resulted lesser record-to-record variability, when compared with the near-fault pulse-like ground motions. However, this difference in the record-to-record variability almost vanished, when different sources of the variabilities (i.e., the modelling, the test data, the design requirement and the damage state threshold) are considered and combined to estimate the total variability, and only marginal differences (up to 10%) in total variability exist, for seismic fragility curves obtained using two different suites of ground motions. As a result, the well comparable seismic fragility curves are obtained using two suites of the ground motions.

• The damage probability matrices and mean loss ratios for the investigated buildings are also observed to be comparable. The negligible differences observed in the estimated mean loss ratios (up to a maximum of 13%, for the investigated buildings and levels of seismic hazard) clearly highlight the potential for the application of the spectrally equivalent ground-motion records, as an alternative to the pulse-like ground-motion records, for seismic fragility and risk assessment in the near-fault sites.

The presented observations are applicable to the height ranges of RC frame buildings considered in the present study. To be able to generalize these observations, the presented work needs to be extended for other building typologies, seismic zones, and building heights as well.

Acknowledgements

The work presented in this manuscript was financially supported by ISIRD Grant (F. No. 9-385/2019/IITRPR/3220) of IIT Ropar. The ground-motion records used in this study were obtained from PEER NGA WEST 2 Database. Author would also like to express his thanks to two anonymous reviewers for very constructive comments and suggestions to improve the manuscript.

References

Akkar, S., Yazgan, U. and Gulkan, P. (2005), "Drift estimates in frame buildings subjected to near-fault ground motions", *J. Struct. Eng., ASCE*, **131**(7), 1014-1024. https://doi.org/10.1061/(ASCE)0733-9445(2005)131:7(1014).

Alavi, B. and Krawinkler, H. (2004), "Behavior of moment-resisting frame structures subjected to near-fault ground motions", *Earthq. Eng. Struct. Dyn.*, **33**(6), 687-706. https://doi.org/10.1002/eqe.369.

Almufti, I., Motamed, R., Grant, D.N. and Willford, M. (2015), "Incorporation of velocity pulses in design ground motions for response history analysis using a probabilistic framework", *Earthq. Spectra*, **31**(3), 1647-1666.

Ambraseys, N. and Douglas, J. (2000), "Reappraisal of the effect of vertical ground motions on response engineering", *ESEE Report No. 00-4*, 1-8.

Ansari, M., Ansari, M. and Safiey, A. (2018), "Evaluation of seismic performance of mid-rise reinforced concrete frames subjected to far-field and near-field ground motions", *Earthq. Struct.*, **15**(5), 453-462. https://doi.org/10.12989/eas.2018.15.5.453 453.

ASCE 41-13 (2013), "Seismic evaluation and retrofit of existing buildings", *Amer. Soc. Civil Eng.*, Reston, Virginia, U.S.A.

Baker, J.W. (2007), "Quantitative classification of near- fault ground motions using wavelet analysis", *Bull. Seismol. Soc. Amer.*, **97**(5), 1486-1501. https://doi.org/10.1785/0120060255.

Baker, J.W. (2011), "Conditional mean spectrum: Tool for ground-motion selection", *J. Struct. Eng., ASCE*, **137**(3), 322-331. https://doi.org/10.1061/(ASCE)ST.1943-541X.0000215.

Baker, J.W. and Cornell, C.A. (2006), "Spectral shape, epsilon and record selection", *Earthq. Eng. Struct. Dyn.*, **35**(9), 1077-1095. https://doi.org/10.1002/eqe.571.

Barbat, A.H., Yépez Moya, F. and Canas, J.A. (1996), "Damage scenarios simulation for seismic risk assessment in urban zones", *Earthq. Spectra*, **12**(3), 371-394.

Bazzurro, P. and Luco, N. (2006), "Damage potential of near-source ground motion records", *The Proc. of the 8th U.S. National Conference on Earthquake Engineering*, San Francisco, California.

BIS (1987a), "Indian standard – Code of practice for design loads (other than earthquake) for buildings and structures (Dead loads)," IS 875 Part 1, Bureau of Indian Standards, New Delhi, India.

BIS (1987b), "Indian standard – Code of practice for design loads (other than earthquake) for buildings and structures (Live Loads)," IS 875 Part 2, Bureau of Indian Standards, New Delhi, India.

BIS (2016a), "Indian standard criteria for earthquake resistant design of structures, Part 1: General provisions and buildings (Fifth revision)," IS 1893 Part 1, Bureau of Indian Standards, New Delhi, India.

BIS (2016b), "Ductile design and detailing of reinforced concrete structures subjected to seismic forces – Code of practice," IS 13920, Bureau of Indian Standards, New Delhi, India.

Bradley, B.A. (2010), "A generalized conditional intensity measure approach and holistic ground-motion selection", *Earthq. Eng. Struct. Dyn.*, **39**(12), 1321-1342. https://doi.org/10.1002/eqe.995.

Carausu, A., and Vulpe, A. (1996), "Fragility estimation for seismically isolated nuclear structures by high confidence low probability of failure values and bilinear regression", *Nuclear Eng. Des.*, **160**, 287-297. https://doi.org/10.1016/0029-5493(95)01108-0.

Champion, C. and Liel A. (2012), "The effect of near-fault directivity on building seismic collapse risk", *Earthq. Eng. Struct. Dyn.*, **41**(10), 1391-1409. https://doi.org/10.1002/eqe.1188.

Chang, Z., Liu, Z., Chen, Z. and Zhai, C. (2019), "Use of near-fault pulse-energy for estimating critical structural response", *Earthq. Struct.*, **16**(4), 415-423. https://doi.org/10.12989/eas.2019.16.4.415.

Chioccarelli, E. and Iervolino, I. (2010), "Near-source seismic demand and pulse-like records: a discussion for L'Aquila earthquake", *Earthq. Eng. Struct. Dyn.*, **39**(9), 1039-1062. https://doi.org/10.1002/eqe.987.

CSI (2016), "ETABS 2016 Integrated building design software, Version 16.0.1", *Comput. Struct*., *Inc*., Berkeley, U.S.A.

Eads, L., Miranda, E. and Lignos, D.G. (2015), "Average spectral acceleration as an intensity measure for collapse risk assessment", *Earthq. Eng. Struct. Dyn.*, **44**(12), 2057-2073. https://doi.org/10.1002/eqe.2575.

Eads, L., Miranda, E. and Lignos, D.G. (2016), "Spectral shape metrics and structural collapse potential", *Earthq. Eng. Struct. Dyn.*, **45**(10), 1643-1659. https://doi.org/10.1002/eqe.2739

FEMA (2002), "Multi-Hazard loss estimation methodology earthquake model", FEMA HAZUS-MH MR 1, Federal Emergency Management Agency, Washington, D.C., U.S.A.

FEMA (2009), "Quantification of seismic performance factors", FEMA P695, Federal Emergency Management Agency, Washington, D.C., U.S.A.

FEMA (2015), "Seismic performance assessment of buildings - Volume 1 methodology," FEMA P58, Federal Emergency Management Agency, Washington, D.C., U.S.A.

Gehl, P., Douglas, J. and Seyedi, D.M. (2015), "Influence of the number of dynamic analyses on the accuracy of structural response estimates", *Earthq. Spectra*, **31**(1), 97-113. https://doi.org/10.1193%2F102912EQS320M.

Haldar, P. and Singh, Y. (2009), "Seismic performance and vulnerability of Indian code designed RC frame buildings", *ISET J. Earthq. Technol.*, **46**(1), 29-45.

Haldar, P., Singh, Y. and Paul, D.K. (2012), "Effect of URM infills on seismic vulnerability of Indian code designed RC frame buildings", *Earthq. Eng. Eng. Vib.*, **11**(2), 233-241. https://doi.org/10.1007/s11803-012-0113-5.

Haselton, C.B., Baker, J.W., Liel, A.B. and Deierlein, G.G. (2011), "Accounting for ground-motion spectral shape characteristics in structural collapse assessment through an adjustment for epsilon", *J. Struct. Eng., ASCE*, **137**(3), 332-344. https://doi.org/10.1061/(ASCE)ST.1943-541X.0000103.

Iervolino, I., Chioccarelli, E. and Baltzopoulos, G. (2012), "Inelastic displacement ratio of near-source pulse-like ground motions", *Earthq. Eng. Struct. Dyn.*, **41**(15), 2351-2357. https://doi.org/10.1002/eqe.2167.

Jaiswal, K., Wald, D. and D'Ayala, D. (2011), "Developing empirical collapse fragility functions for global building types", *Earthq. Spectra*, **27**(3), 775-795.

Jayaram, N., Lin, T. and Baker, J.W. (2011), "A computationally efficient ground-motion selection algorithm for matching a target response spectrum mean and variance", *Earthq. Spectra*, **27**(3), 797-815. https://doi.org/10.1193%2F1.3608002.

Kappos, A.J. and Panagopoulos, G. (2010), "Fragility curves for reinforced concrete buildings in Greece", *Struct. Infrastruct. Eng.*, **6**(1-2), 39-53. https://doi.org/10.1080/15732470802663771.

Kappos, A.J., Stylianidis, K.C. and Pitilakis, K. (1998), "Development of seismic risk scenarios based on a hybrid method of vulnerability assessment", *Nat. Haz.*, **17**(2), 177-192. https://doi.org/10.1023/A:1008083021022.

Kim, S.H. and Shinozuka, M. (2004), "Development of fragility curves of bridges retrofitted by column jacketing", *Probabil. Eng. Mech.*, **19**(1-2), 105-112. https://doi.org/10.1016/j.probengmech.2003.11.009.

Kohrangi, M., Vamvatsikos, D. and Bazzurro, P. (2019), "Pulse-like versus non pulse-like ground motion records: Spectral shape comparisons and record selection strategies", *Earthq. Eng. Struct. Dyn.*, **48**(1), 46-64. https://doi.org/10.1002/eqe.3122.

Kumar, A., Mittal, H., Sachdeva, R. and Kumar, A. (2012), "Indian strong motion instrumentation network", *Seismol. Res. Lett.*, **83**(1), 59-66. https://doi.org/10.1785/gssrl.83.1.59.

Kumar, P., Kumar, A. and Pandey, A.D. (2016), "Spectral characterization of Himalayan near-fault ground motion", *Periodica Polytech. Civil Eng.*, **60**(2), 205-215. https://doi.org/10.3311/PPci.7754.

Lang, D.H. (2013), "*Earthquake damage and loss assessment – Predicting the unpredictable*", Ph.D. Dissertation, University of Bergen, Norway.

Mansouri, I., Shahbazi, S., Hu, J.W. and Moghaddam, S.A. (2019), "Effect of pulse-like nature of forward directivity ground-motions on seismic behaviour of steel moment frames", *Earthq. Struct.*, **17**(1), 1-15. https://doi.org/10.12989/eas.2019.17.1.001.

Maqsood, T., Edwards, M., Ioannou, I., Kosmidis, I., Rossetto, T. and Corby, N. (2016), "Seismic vulnerability functions for Australian buildings by using GEM empirical vulnerability assessment guidelines", *Nat. Haz.*, **80**(3), 1625-1650. http://10.1007/s11069-015-2042-x.

Mavroeidis, G.P., Dong, G. and Papageorgiou, A.S. (2004), "Near-fault ground motions, and the response of elastic and inelastic single-degree-of-freedom (SDOF) systems", *Earthq. Eng. Struct. Dyn.*, **33**(9), 1023-1049. https://doi.org/10.1002/eqe.391.

Meslem, A., D'Ayala, D., Ioannou, I., Rossetto, T. and Lang D. H. (2014), "Uncertainty and quality rating in analytical vulnerability assessment", *The Second European Conference of Earthquake Engineering and Seismology*, Istanbul.

Rossetto, T. and Elnashai, A.S. (2003), "Derivation of vulnerability functions for European-type RC structures based on observational data", *Eng. Struct.*, **25**, 1241-1263. https://doi.org/10.1016/S0141-0296(03)00060-9.

Rossetto, T. and Elnashai, A.S. (2005), "A new analytical procedure for the derivation of displacement-based vulnerability curves for populations of RC structures", *Eng. Struct.*, **27**, 397-409. https://doi.org/10.1016/j.engstruct.2004.11.002.

Ruiz-Garcia, J. (2011), "Inelastic displacement ratios for seismic assessment of structures subjected to forward directivity near-fault ground-motions", *J. Earthq. Eng.*, **15**(3), 449-468. https://doi.org/10.1080/13632469.2010.498560.

Shahi, S.K. and Baker, J.W. (2014), "NGA-West2 models for ground-motion directionality", *Earthq. Spectra*, **30**(3), 1285-1300. https://doi.org/10.1193%2F040913EQS097M.

Singhal, A. and Kiremidjian, A.S. (1996), "Method for probabilistic evaluation of seismic structural damage", *J. Struct. Eng., ASCE*, **122**(12), 1459-1467. https://doi.org/10.1061/(ASCE)0733-9445(1996)122:12(1459).

Somerville, P.G., Smith, N.F., Graves, R.W. and Abrahamson, N. A. (1997), "Modification of empirical strong ground motion attenuation relations to include the amplitude and duration effects of rupture directivity", *Seismol. Res. Lett.*, **68**(1), 199-222. https://doi.org/10.1785/gssrl.68.1.199.

Stewart, J., Chiou. S-J., Bray, J.D., Graves, R.W., Somerville, P.G. and Abrahamson, N.A. (2002), "Ground motion evaluation procedures for performance- based design", *Soil Dyn. Earthq. Eng.*, **22**(9-12), 765-772. https://doi.org/10.1016/S0267-7261(02)00097-0.

Surana, M. (2019), "Evaluation of seismic design provisions for acceleration-sensitive non-structural components", *Earthq. Struct.*, **16**(5), 611- 623. https://doi.org/10.12989/eas.2019.16.5.611.

Surana, M., Meslem, A., Singh, Y. and Lang, D.H. (2020), "Analytical evaluation of damage probability matrices for hill-side RC buildings using different seismic intensity measures", *Eng. Struct.*, **207**, https://doi.org/10.1016/j.engstruct.2020.110254.

Surana, M., Singh, Y. and Lang, D.H. (2018), "Seismic characterization and vulnerability of building stock in hilly regions", *Nat. Haz. Rev., ASCE*, **19**(1), 04017024. https://doi.org/10.1061/(ASCE)NH.15276996.0000275.

Tothong, P. and Cornell, C.A. (2008), "Structural performance assessment under near-source pulse-like ground motions using advanced ground motion intensity measures", *Earthq. Eng. Struct. Dyn.*, **37**(7), 1013-1037. https://doi.org/10.1002/eqe.792.

Wood, H.O. and Neumann, F. (1931), "Modified Mercalli intensity scale of 1931", *Bull. Seismol. Soc. Amer.*, **21**(4), 277-283.

Zamora, M. and Riddell, R. (2011), "Elastic and inelastic response spectra considering near-fault effects", *J. Earthq. Eng.*, **15**(5), 775-808. https://doi.org/10.1080/13632469.2011.555058.

Zentner, I. (2010), "Numerical computation of fragility curves for NPP equipment", *Nuclear Eng. Des.*, **240**, 1614-1621. https://doi.org/10.1016/j.nucengdes.2010.02.030.

KT